

Synthesis And Characterization Of Zeolite A From Aloji Kaolin Via Hydrothermal Method

ABSTRACT

This study focused on the synthesis and characterization of Zeolite A from Aloji kaolin via the hydrothermal method. The effect of short crystallization times (0.5h, 1h, 1.5h, 2h, and 3h) and high crystallization temperature of 115 °C on the formation of Zeolite A as the final product was investigated. The characterization of the synthesized Zeolite A was conducted using a Scanning electron microscope (SEM), X-ray diffraction (XRD), and Brunauer-Emmett-Teller (BET) analysis. The results showed a well-developed Zeolite A with cubic morphology and a crystallinity of 78.12%, as well as a surface area and pore size of 18.8832 m²/g and 178.461 Å respectively was successfully synthesized using high alkali concentration (5 mol/L) and a crystallization time of 3h. The findings provide valuable insight into the synthesis of Zeolite A from kaolin and its potential application in various fields.

Keywords: [Kaolin, Zeolite, Crystallization, Temperature, Hydrothermal]

1. INTRODUCTION.

The increase in global population as well as rapid industrialization has resulted in the depletion of non-renewable resources, increasing pollution, and thus various ecological and environmental problems. These problems have greatly transcended to the degradation of the environment and human health which has greatly caused people to become inquisitive about the current model of industrialization procedure and production. Due to improvements in regulations and the emergence of new policies, there is a shift in the regular mode of pollution first then treatment later to a cleaner method of production. In the clean production methods harmful and very toxic substances that cause pollution are either avoided or reduced to the barest minimum [1].

Zeolites are microporous, nontoxic, and crystalline aluminosilicate materials that are formed by a three-dimensional network of silica [SiO₄]⁴⁻ and alumina [AlO₄]⁵⁻ tetrahedron having shared oxygen atoms [2-3]. The zeolite's tetrahedral structure comprises a well-organized network of channels, pores, and cavities with molecular dimensions that can be filled with exchangeable cations or water molecules [4-5]. Zeolites commonly referred to as molecular sieves possess uniformly sized pores and find extensive use in diverse applications including catalysis, bacterial adhesion, adsorption processes, water treatment, air pollution control, detergent manufacturing, fuel cells, and ion exchange [3, 6-8].

Zeolites exist in typically two main types namely natural and synthetic. Natural zeolites are mined from sedimentary rocks in the earth whereas synthetic types are manufactured in laboratories. The most common types of natural zeolites include Laumontite, Clinoptilolite, Heulandite, Analcime, Chabazite, and Mordenite [9-10]. These natural zeolites contain various impurities like SO₄²⁻, Fe²⁺, SiO₂, and other zeolites thereby making them unfit for use in fields

where uniformity and purity are essential. However, due to the significant demand for zeolite and the expensive nature of purifying natural zeolite, synthetic zeolite materials were developed [3, 11]. Synthetic zeolites are typically favored because of their uniform composition (particle size and shape) and high crystallinity, which surpasses that of natural zeolites. This is primarily because structural properties and chemical compositions can be easily controlled by adjusting synthesis parameters during production [12-13].

The preparation and synthesis of synthetic zeolites are highly challenging, and the typical methods of synthesis involve using alumina and silica obtained from analytical/ synthetic chemicals to form aluminosilicate hydrogel which is then crystallized to obtain zeolite. This source of alumina and silica is very expensive and leads to a high cost of zeolite in addition to causing several environmental burdens due to pollution from the use of analytical-grade chemicals [11,14-15]. To eliminate these limitations researchers have been prompted to investigate the synthesis of synthetic zeolite using several other alternative sources such as bauxite [16], clay [17-18], and coal fly ash [19]. Natural clays are readily available, cheap and very abundant, when compared to other sources of silica as such they are most frequently used for production of mesoporous silica. Kaolin is an alternative source for alumina and silica because of its low-cost benefit and it has a Si/Al ratio of 1 which is suitable for the synthesis of low silica zeolites. [2,13,20]. Low silica zeolites such as zeolite A, are particularly intriguing because of their exceptional adsorption and ion exchange capabilities [5,21-22]. In general, zeolite synthesis using kaolin as starting material typically involves two stages namely: metakaolinization (the calcination of the raw kaolin at elevated temperature to obtain an amorphous, chemically reactive and stable metakaolin) and hydrothermal treatment of metakaolin with sodium hydroxide [12]. The hydrothermal treatment/method is a conventional method for zeolite synthesis from kaolin. This method is carried out in two main steps: (a) dissolution of meta-kaolin in an alkali solution to form homogenous gel, and (b) crystallization of zeolites in autoclave [18].

In this work, Aloji kaolin was used as an alternative source for alumina and silica because of its low-cost benefit and it has a Si/Al ratio of 1 which is suitable for the synthesis of low silica zeolites. The work involves the synthesis of zeolite A from Aloji kaolin. This will be achieved by refining raw kaolin and then converting this to metakaolin by calcination. The metakaolin will then be used in synthesizing zeolite A.

2. MATERIAL AND METHODS

2.1 Materials

Raw Kaolin was obtained from Aloji in Kogi state, Nigeria. The only chemical reagent used was an analytical grade sodium hydroxide (NaOH) pellet of 97% purity obtained from Sigma Aldrich. Also, deionized and distilled water were all obtained from the Laboratory in Chemical Engineering Department of the Federal University of Technology, Minna, and the water was used as received.

2.2 Synthesis of Zeolite A

Zeolite A was synthesized from Aloji Kaolin using the conventional hydrothermal method. Raw Aloji kaolin was crushed mildly and sieved using an 850 μ m sieve mesh. This was then transferred into a 1000ml beaker where it was soaked using deionized water for 12h. The mixture was then stirred continuously for about 30 minutes after which the lighter fraction (supernatant) was collected. After sedimentation, the Kaolin was decanted and dried in the oven. The obtained refined Aloji Kaolin was then calcined in a furnace at 850 $^{\circ}$ C for 2h to obtain metakaolin which is a more reactive form of Kaolin. Metakaolin was mixed with a 5 M concentration of sodium hydroxide (NaOH) and the resulting mixture was stirred using a magnetic stirrer. The homogenous solution was aged and then heated in a Teflon-lined

stainless-steel autoclave at 115 °C for various crystallization times of 0.5 h, 1 h, 1.5 h, 2 h, and 3 h. The resultant product obtained was continuously washed with deionized water to obtain a pH of 8.5, after which the synthesized zeolite sample was dried in an oven at 100 °C for 8 h and the zeolite crystals obtained were stored in an air-tight container.

2.3 Material Characterization

The Aloji kaolin clay underwent X-ray Fluorescence (XRF) analysis using an XRF-1800 Shimadzu, Japan to determine its chemical composition in terms of metal oxides. Additionally, X-ray Diffraction (XRD) analysis was conducted to determine the mineralogical phases and crystalline for the kaolin clay, metakaolin, and synthesized zeolite A using an Ultima IV instrument from Rigaku, UK, utilizing Cu-K α ($\lambda=0.154$) radiation with a fixed power source (40 kV, 40 mA). The diffraction angle (2θ) ranged from 5 to 90 degrees. Furthermore, their particle morphologies were examined using high-resolution SEM techniques with a FEI Quanta 400 instrument. The surface properties of these materials were investigated through BET analysis using Chem BET 3000, USA.

3. RESULTS AND DISCUSSION

3.1 X-ray Fluorescence (XRF) for Aloji Kaolin

The XRF analysis of the raw kaolin clay is detailed in Table 1, revealing that Aloji kaolin primarily comprises 46.42% SiO₂ and 38.76% Al₂O₃. This composition aligns with previous studies by Dewi et al. [23], Lim et al. [13], and Adeniyi et al. [24], which also found that kaolin clay predominantly consists of SiO₂ and Al₂O₃. These components, alumina, and silica are essential constituents for the formation of zeolites. Aloji kaolin exhibits a SiO₂/Al₂O₃ ratio of 1.97 and a Si/Al ratio of 0.98, indicating its suitability for synthesizing zeolite A. Comparatively, the studies by Lim et al. [13] and Adeniyi et al. [24] reported SiO₂/Al₂O₃ ratios of 2.086 and 1.24 respectively, demonstrating slight variations likely due to differences in the kaolin sources.

Table 1: Percentage chemical composition of kaolin based on XRF Analysis

Compound	Value (Wt%)		
	This Work	Lim et al. [13]	Adeniyi et al. [24]
SiO ₂	46.42	45.42	49.20
Al ₂ O ₃	38.76	36.94	39.80
Na ₂ O	1.56	0.00	-
B ₂ O ₃	1.02	-	-
MgO	1.33	0.53	-
K ₂ O	0.52	3.96	0.33
TiO ₂	0.80	0.08	-
Fe ₂ O ₃	3.15	0.36	2.90
FeO	1.25	-	-
MnO	1.17	0.03	0.04
Cr ₂ O ₃	0.05	-	0.04
NiO	0.13	-	0.09

P ₂ O ₅	0.27	0.01	0.36
CaO	1.52	1.68	0.04

3.2 XRD ANALYSIS

The XRD pattern for Alojji Kaolin is shown in Figure 1. The pattern shows diffraction peaks at 2θ values of 9.3, 12.66, 21.29, 25.20, 27.0, 36.95, 39.87, and 42.80°. The kaolinite peaks are evident at 2θ values of 12.66, 25.20, 36.95, and 39.62 while other crystalline phases such as quartz and mica are found at 2θ values of 21.29 and 27.0°. Similar peaks were reported by Dewi et al. [23] and Lim et al. [13]. In zeolite synthesis using kaolin, shifts and changes in peak intensities were mostly observed within the kaolinite peaks, thus indicating that kaolin can be readily converted into sodium silicate and sodium aluminium silicate, and then finally zeolite. The metakaolinization process converted crystalline inactive kaolinite to amorphous reactive metakaolin having only a slight quartz peak as the crystalline phase present.

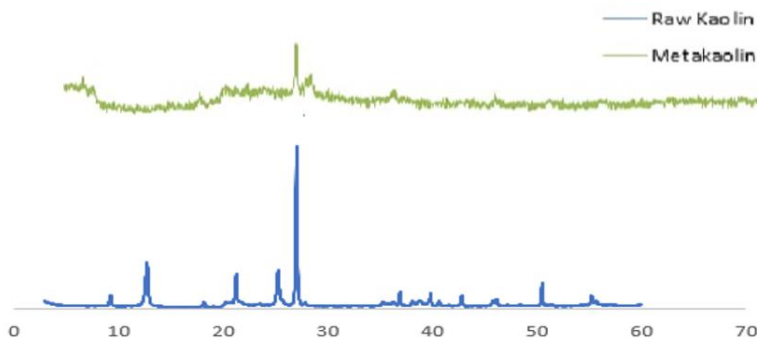


Figure 1. XRD pattern for kaolin and metakaolin

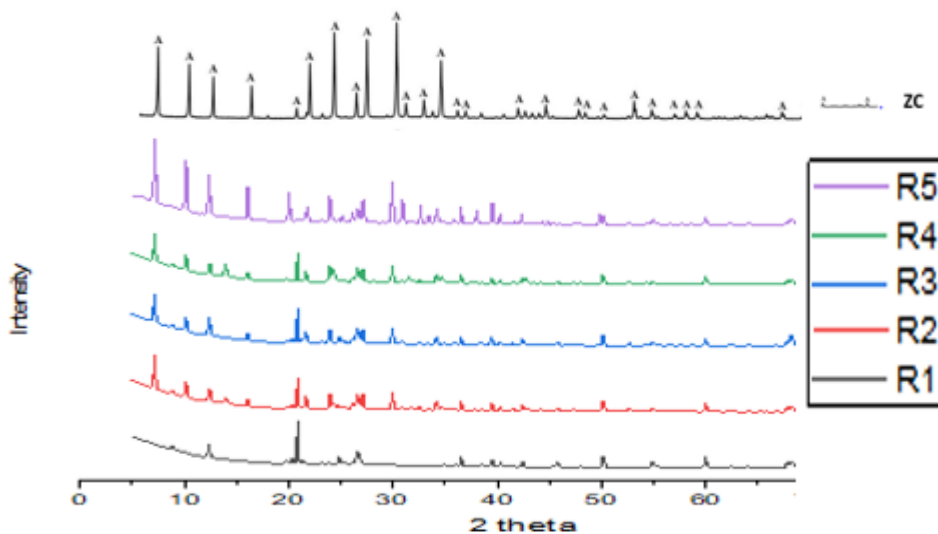


Figure 2. XRD pattern for synthesized zeolite at various crystallization times

In the study of zeolite synthesis, XRD analysis was carried out. Figure 2 shows the XRD pattern for the zeolite synthesized at various crystallization times. It can be seen from the result that the XRD obtained after 0.5 h of crystallization (R1) showed peaks at 2 theta values of 12.51, and 24.64 and quartz peaks at 26.67. However, at a crystallization time of 1 h as indicated by plot R2, other diffraction peaks became visible. Here peaks characteristic of zeolite A (as seen from the XRD pattern of commercial zeolite ZC) began to emerge. The diffraction peaks at 2 Θ values of 7.18, 10.24, 12.49, 16.04, 20.46, 30.89, and 34.21 were obtained. Similarly, a peak characteristic of faujesite was obtained at a 2 Θ value of 14.21; this readily disappeared as crystallization time increased to 1.5 h. The diffraction peaks obtained at 1.5 h (R3) have similar peaks as those at 1h. it was observed that more peaks characteristic of zeolite A were added and the faujesite peak disappeared. New peaks that emerged at 1.5 h were obtained at 2 Θ values of 19.98, 24.13, 36.67, 39.65, 42.31 and 42.74. The diffraction peaks obtained after 2 h (R4) crystallization time were seen at 2 theta values of 7.18, 10.24, 12.49, 16.04, 20.46, 24.13,30.89, 34.21, 36.67, 39.65, 42.31, 42.74. 44.25 and 47.34. These peaks are characteristic peaks obtained for zeolite A according to Tracey and Haggins [25]. This confirms that zeolite A formation begins even after 1h crystallization time and continues to new peaks emerging with increasing time. The peaks obtained for zeolite synthesized at 3 h in this study gave the highest crystallinity of 78.12 % and the diffraction peaks were observed at 2 Θ values of 7.18, 10.24, 12.49, 16.04, 20.46, 21.71, 24.04, 25.15, 30.01, 30.89, 32.68, 34.21, 36.64, 38.04, 39.62, 40.27, 42.38, 44.20, 44.85, and 49.83. These peaks obtained from this work were in close agreement with that obtained from the works of Yusriadi et al. [26]; Maia et al. [27]and Vegree et al. [28]. Furthermore, it can be seen from Figure 3. that diffraction peaks obtained from the zeolite crystallized at 3 h had peaks of higher intensities than the other zeolites synthesized, this may explain the reason for a higher percentage crystallinity obtained by this zeolite.

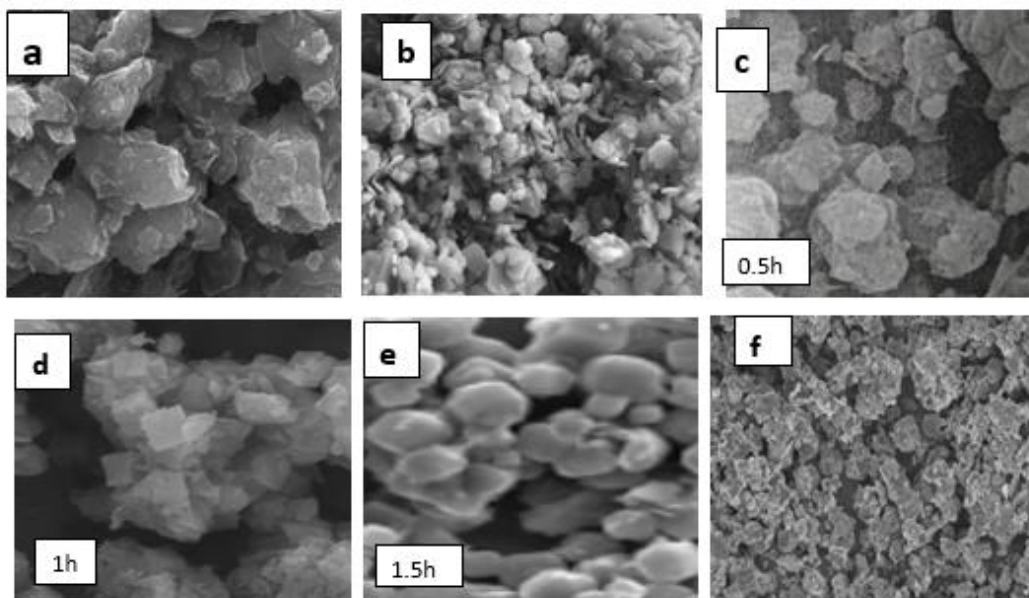


Figure 3: SEM images for a) Kaolin b) Metakaolin (c-g) Zeolite A obtained at (0.5-2 h) crystallization times

3.2. SEM ANALYSIS

The refined kaolin, metakaolin, and zeolite samples synthesized at various crystallization temperatures were analyzed using high resolution SEM. The morphologies obtained for each sample are shown in Figure 3. The micrographs shown in Figure 3a-f give the for the changes in the morphology of kaolin, metakaolin, and zeolite during synthesis. It was observed from Figure 3a that the morphology of kaolin is an assemblage of hexagonal plate-like structures having heterogeneous sizes, while metakaolin also shows flat plated particles having various sizes. This morphology agrees with the work of Lim et al. [13]

The zeolite sample synthesized at various times (0.5-2h) crystallization time is shown in Figure 3c-f. The micrograph in Figure 3c still depicted dominantly flat plated hexagonal shaped morphology having some gel-like substance. The micrograph in Figure 3d gives the zeolite sample formed at 1 h crystallization time. The image shows a mixture of both cubic and hexagonal-shaped morphology for samples. However, the micrograph also showed an improvement from the originally flat-plated metakaolin to a transforming cubic shape [29]. Similarly, it agrees with the XRD result that at this crystallization time peaks characteristic of zeolite were formed, since cubic shaped crystals were observed. Furthermore, in Figure 3e for 1.5 h crystallization time a similar pattern was identified as samples were seen to contain crystals of both cubic and hexagonal crystals. In Figure 3f, the micrographs showed crystals that have predominantly cubic morphology, with very few flat-plated and hexagonal-shaped crystals present. The XRD result obtained confirms that zeolite samples crystallized for 2 h produced more peaks that are characteristic of zeolite A than those crystallized at a lesser time. The micrograph was almost similar to that of the zeolite sample crystallized at 3 h. Although the sample crystallized at 3h showed better-formed cubes. This is clearly shown in Figure 4. The morphology of the synthesized zeolite A after 3 h crystallization time with higher magnification is shown in Figure 4. The micrograph depicts some well-developed cubic crystals that are typical of zeolite A. This shape conforms with Kirdeciler and Akata [21] and Salimkhani et al. [30] who reported obtaining image cubic morphology for zeolite A using kaolin as the starting raw material.

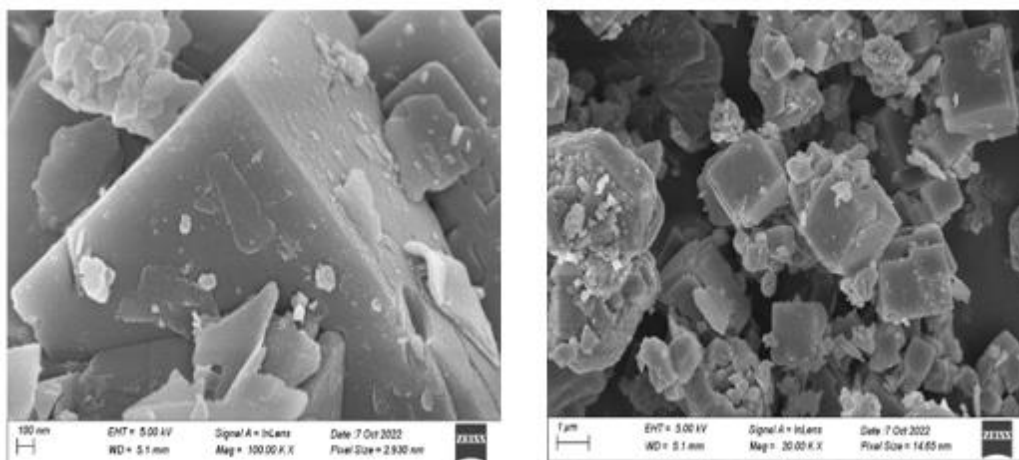


Figure 4: SEM images for zeolite A obtained at 3h crystallization time.

3.3 BET RESULTS

Kaolin and zeolite A synthesized was analyzed to determine the specific surface area, pore size, and specific pore volume using the Brunauer-Emmett-Teller (BET) method. The BET adsorption-desorption isotherm for both Alojji kaolin and zeolite A synthesized is shown in Figure 5. The adsorption isotherm in comparison to International Union of Pure and Applied

Chemistry (IUPAC) classifications corresponds adequately to type IV for both kaolin and synthesized zeolite A. The curves exhibit an abrupt increase, with a convex shape curve at the low relative pressure ratios that results from very strong interactions on the silica surfaces.

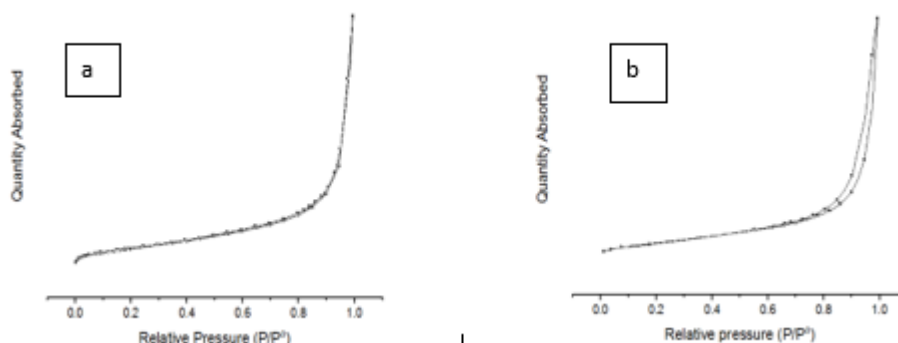


Figure 5: The Adsorption-Desorption isotherm for (a) kaolin and (b) zeolite A

The BET results obtained indicate that Aloji kaolin has a surface area, pore size, and specific pore volume values of $14.15 \text{ m}^2/\text{g}$, 166.593 \AA , and $0.001326 \text{ cm}^3/\text{g}$ respectively. However, for the synthesized zeolite A, the BET analysis showed the values of $18.8832 \text{ m}^2/\text{g}$ for surface area, 178.461 \AA for pore size, and $0.028064 \text{ cm}^3/\text{g}$ for pore volume. These values represent significant improvements compared to those observed for refined kaolin, highlighting the effectiveness of the synthesis process in enhancing the surface area, pore size, and pore volume of the resulting zeolite A. This outcome is consistent with previous findings by Otieno et al. [14] who reported a surface area of $18 \text{ m}^2/\text{g}$ for zeolite A synthesized from kaolin using a hydrothermal method. Furthermore, the surface area achieved in this study surpasses the values of $11.85 \text{ m}^2/\text{g}$ and $17.39 \text{ m}^2/\text{g}$ reported by Vegere et al. [28] and Jin et al. [22] respectively. However, it is noted that the surface area of the synthesized zeolite A appears lower than the $25.3 \text{ m}^2/\text{g}$ reported by Foroughi et al. [20].

4. CONCLUSION

In conclusion, the present study has demonstrated the successful synthesis of zeolite A from Aloji kaolin via hydrothermal method. The effect of varying crystallization times and temperature on the synthesis of zeolite A was investigated, and it was found that a crystallization time of 3 h on an alkali concentration of 5 mol/L resulted in a well-developed zeolite A crystal with high crystallinity and desirable morphological and textural properties. The characterization results obtained through XRD, SEM, and BET analysis confirmed the formation of Zeolite A with a cubic morphology, high surface area, and pore size. These findings suggest that Aloji kaolin can serve as a potential source of raw material for the synthesis of zeolite A which could have potential applications in various fields such as catalysis, separation, and adsorption.

LIST OF ABBREVIATIONS.

SEM: Scanning Electron Microscope

XRD: X-ray Diffraction

BET: Brunauer- Emmett- Teller

XRF: X-ray Fluorescence

REFERENCES

- [1] He, Y., Tang, S., Yin, S., & Li, S. Research progress on green synthesis of various high-purity zeolites from natural material-kaolin. *Journal of Cleaner Production*, 306 (2021) 127248.
- [2] Binay, M.I., Kirdeciler, S.K., & Akata, B. Development of antibacterial powder coatings using single and binary ion-exchanged zeolite A prepared from local kaolin. *Applied Clay Science*, 2019; 182, 1-9. <https://doi.org/10.1016/j.clay.2019.1052>
- [3] Derbe, T., Temesgen, S., and Bitew, M. A Short Review on Synthesis, Characterization, and Applications of Zeolites. *Advances in Materials Science and Engineering*. 2021; <https://doi.org/10.1155/2021/6637898>
- [4] Olaremu, A.G., Odebunmi, E.O., Nwosu, F.O., Adeola, A.O. & Abayomi, T.G. Synthesis of Zeolite from Kaolin Clay from Erusu Akoko Southwestern Nigeria. *Journal for Chemical Society of Nigeria*, 2018; 43 (3), 381-786.
- [5] Kamyab, S. M., & Williams, C. D. Pure zeolite LTJ synthesis from kaolinite under hydrothermal conditions and its ammonium removal efficiency. *Microporous and Mesoporous Materials*. 2021; 318, 111006
- [6] Johnson, E. B. G. & Arshad, S.E. Hydrothermally synthesized zeolites based on kaolinite: A review. *Applied Clay Science*. 2014; 97–98, 215–221
- [7] Albert, A. C., Asadu, C.O., & Abuh, M.A. Synthesis of Zeolite by Thermal Treatment Using Locally Sourced Ugwaka Clay (Black Clay). *Journal of Materials Science Research and Reviews*, 2018; 1 (2), 1-12. DOI: 10.9734/JMSRR/2018/42862
- [8] Hartati, Prasetyoko, D., Mardi Santoso, M., Qoniah, I., Leaw, W. L., Firda, P. B. D., and Nur, H. A review on synthesis of kaolin-based zeolite and the effect of impurities. *Journal of the Chinese Chemical Society*. 2020; 1–26.
- [9] Tasić, Z.Z., Bogdanović, G.D., & Antonijević, M.M. Application of Natural Zeolite in Wastewater Treatment –A Review. *Journal of Mining and Metallurgy*. 2019; 55 A (1) 67-79. doi: 10.5937/JMMA1901067T
- [10] Nasief, F.M., Shaban, M., Alamry, K.A., Abu Khadra, M.R., Khan, A.A.P., Asiri, A.M., & Abd El-Salam, H.M. Hydrothermal synthesis and mechanically activated zeolite material for utilizing the removal of Ca/Mg from aqueous and raw groundwater. *Journal of Environmental Chemical Engineering*, 2021; 9, 105834
- [11] Yoldi, M., Fuentes-Ordonez, E.G., Korili, S.A., & Gil, A. Zeolite synthesis from industrial wastes. *Microporous and Mesoporous Materials*, 2019; 287, pp 183–191.
- [12] Aragaw, T. A., & Ayalew, A. A. Removal of water hardness using zeolite synthesized from Ethiopian kaolin by hydrothermal method. *Water Practice & Technology*, 2019; 14 (1), 145-159. doi: 10.2166/wpt.2018.116.
- [13] Lim, W., Lee, C., & Hamm. S. Synthesis and characteristics of Na-A zeolite from natural kaolin in Korea. *Materials Chemistry and Physics*, 2021; 261, 124230

- [14] Otieno, S.O., Kengara, F.O., Kemmegne-Mbougouen, J.C., Langmi, H.W., Kowenje, C.B.O., & Mokaya, R. The effects of metakaolinization and fused-metakaolinization on zeolites synthesized from quartz-rich natural clays. *Microporous and Mesoporous Materials*, 2019; 290, 109668
- [15] Kumar, M.M & Jena, H. Direct single-step synthesis of phase pure zeolite Na-P1, hydroxy sodalite, and analcime from coal fly ash and assessment of their Cs⁺ and Sr²⁺ removal efficiencies. *Microporous and Mesoporous Materials*, 2022; 333, 111738.
- [16] Rahman, A., Ur Rehman, W., Khan, F.U., & Shah. J. Synthesis of Zeolite 4A Using Bauxite as Aluminum Source: Characterization and Performance. *Journal of Chemical Technology and Metallurgy*, 2021; 56, 2, 327-330.
- [17] Srilal, S., Tanwongwan, W., Onpetch, K., Wongkitikun, T., Panpiemrasda, K., Panomsuwan, G., & Eiad-ua, A. *Synthesis of zeolite A from bentonite via hydrothermal method: The case of different base solution*. The Second Materials Research Society of Thailand International Conference AIP Conference Proceedings 2279, 2020; 060006-1–060006-6; <https://doi.org/10.1063/5.0025043>
- [18] Arasi, M. A., Salem, A., & Salem, S. Production of Mesoporous and Thermally Stable Silica Powder from Low Grade Kaolin Based on Eco-Friendly Template free Route via Acidification of Appropriate Zeolite Compound for Removal of Cationic Dye from Wastewater. *Sustainable Chemistry and Pharmacy* 2021; 19, 1-10. <https://doi.org/10.1016/j.scp.2020.100366>
- [19] Yang L, Qian X, Yuan P, Bai H, Miki T, Men F, Li H, & Nagasaka T. Green synthesis of zeolite 4A using fly ash fused with synergism of NaOH and Na₂CO₃. *Journal of Cleaner Production*, 2019; doi: <https://doi.org/10.1016/j.jclepro.2018.11.259>.
- [20] Foroughi, M., Salema, A., & Salem, S. Characterization of phase transformation from low grade kaolin to zeolite LTA in fusion technique: Focus on quartz melting and crystallization in presence of NaAlO₂, *Materials Chemistry and Physics*, 2021; 258, 1-9. <https://doi.org/10.1016/j.matchemphys.2020.123892>
- [21] Kirdeciler, S. K. & Akata, B. One pot fusion route for the synthesis of zeolite 4A using kaolin. *Advanced Powder Technology*, 2020; 31, 4336–4343. <https://doi.org/10.1016/j.apt.2020.09.012>
- [22] Jin, Y., Li, L., Liu, Z., Zhu, S., & Wang, D. Synthesis and characterization of low-cost zeolite NaA from coal gangue by hydrothermal method. *Advanced Powder Technology*, 2021; 32, 791–801. <https://doi.org/10.1016/j.apt.2021.01.024>
- [23] Dewi, R., Agusnar, H., Alfian, Z., & Tamrin. Characterization of technical kaolin using XRF, SEM, XRD, FTIR and its potentials as industrial raw materials *Journal of Physics: Conference Series*, 2018; 1116, 1-7. doi:10.1088/1742-6596/1116/4/042010.
- [24] Adeniyi, F. I., Ogundiran, M. B., T. Hemalatha, T., & Hanumantrai, B. B. Characterization of raw and thermally treated Nigerian kaolinite-containing

clays using instrumental techniques *Springer Nature Applied Sci*, 2020; 2, 821-829 <https://doi.org/10.1007/s42452-020-2610-x>

- [25] Treacy, M.M.J & Higgins, J.B. Collection of simulated XRD powder patterns of zeolites. Fourth revised edition, *Amsterdam Elsevier*. 2001; 379
- [26] Yusriadi, Y., Sulastri, E., & Lembang, N. Synthesis of Type A Zeolite from Rice Husk Ash and Its Application as a Builder on Effervescent Tablet Form Detergent. *Tenside Surfactant Detergent*, 2020; 57, 3.
- [27] Maia, A. B., Dias, R. N., Rômulo, S. A., and Neves, R.F. Influence of an aging step on the synthesis of zeolite NaA from Brazilian Amazon kaolin waste. *Journal of Material Research and Technology*; 2019; 8(3):2924–2929
- [28] Vegree, K., Kravcevic, R., Krauklis, A.E., & Juhna, T. Comparative study of hydrothermal synthesis routes of zeolite A. *Materials Today: Proceedings*, 2020; <https://doi.org/10.1016/j.matpr.2020.06.326>
- [29] Gougazeh, M & Buhl, J. Synthesis and characterization of zeolite A by the hydrothermal transformation of natural Jordanian kaolin. *Journal of the Association of Arab Universities for Basic and Applied Sciences*. 2014; 15, pp.35–42
- [30] Salimkhani, S., Siahcheshm, K., Kadkhodaie, A., & Salimkhani, H. Structural analysis and the effect of the chromium on LTA (Na) zeolite synthesized from kaolin. *Materials Chemistry and Physics*, 2021; 271, 124957.

UNDER PEER REVIEW